Crystallization and Intriguing Morphologies of Compatible Mixtures of Tetrahydrofuran−Methyl Methacrylate Diblock Copolymer with Poly(tetrahydrofuran)

Li-Zhi Liu,* Wei Xu, Hong Li, Fengyu Su, and Enle Zhou

Polymer Physics Laboratory, Changchun Institute of Applied Chemistry, Chinese Academy of Sciences, Changchun, 130022, P. R. China

Received May 9, 1996; Revised Manuscript Received December 2, 1996[⊗]

ABSTRACT: The crystallization and unusual crystalline morphologies of compatible mixtures of tetrahydrofuran−methyl methacrylate diblock copolymer with tetrahydrofuran homopolymer were studied. It is shown that the PTHF [poly(tetrahydrofuran)] block of the copolymer cocrystalizes with the PTHF homopolymer in the PTHF microphase of the blend. However, the degree of crystallinity of the PTHF block is always lower than that of the PTHF homopolymer in the PTHF microphase. The crystallizability of the PTHF microphase increases appreciably with increasing PTHF microphase size and PTHF homopolymer weight fraction in the microphase. The morphology study of the blends shows that the crystalline morphology is strongly dependent on blend composition, copolymer composition and PTHF block length, as well as crystallization temperature. When alternating PTHF and PMMA [poly(methyl methacrylate)] lamellae are formed, the macroscopic crystalline morphology could be only observed when the thickness of the PTHF lamellae is large enough (∼20 nm). In the blend where PMMA spherical or cylindrical microphases are formed, the crystalline morphology changes dramatically with the change in the PTHF microdomain size and PMMA interdomain distance. Many unusual crystalline morphologies have been observed. A study of the solution-crystallized morphology of the blends at different temperatures shows that the morphology is also strongly dependent on the isothermal crystallization temperature, suggesting that the PMMA microdomains may have different effects on the morphology formation when the blend is crystallized at different rates.

Introduction

The compatibility and microphase separation of mixtures of an amorphous diblock copolymer AB with its corresponding homopolymer A have been extensively studied both experimentally[1−4] and theoretically.[5−7] The compatibility of the AB/A blends is dependent on the molecular weight ratio of the homopolymer A to the block A of the copolymer. The smaller the ratio, the better the compatibility of the blend. In such blends, spherical, cylindrical, lamellar, hexagonally-perforated (catenoid) lamellar, bicontinuous $Ia\bar{3}d$ cubic (gyroid) and bicontinuous $Pn\bar{3}m$ cubic (double diamond) microphases[1−5] can be formed, depending on the blend composition, the copolymer composition, and the temperature. Therefore, in AB/A compatible blends with one of the two blocks being crystallizable, the crystallization behavior, the structure, and the morphology could be very different from the extensively studied miscible semicrystalline/amorphous homopolymer blends due to the influence of these microphases. MacKnight[8] *et al*. recently reported their study on the crystallization kinetics of mixtures of a symmetric poly(ethylene-*b*-atactic propylene) diblock copolymer with atactic polypropylene by using the differential scanning calorimetry (DSC) technique. Nojima[9] *et al*. studied the morphology in the binary blends of an ϵ-caprolactone−butadiene diblock copolymer (PCL-*b*-PB) with poly(ϵ-caprolactone) by using a small angle X-ray scattering (SAXS) technique. In our earlier preliminary work[10] about the mixtures of a (semicrystalline) tetrahydrofuran-*b*-methyl methacrylate diblock copolymer (PTHF-*b*-PMMA) with (semicrystalline) PTHF homopolymers, the crystallization behavior and crystalline morphological features of the compatible and incompatible PTHF-*b*-PMMA/PTHF blends were studied. The microphase separation and crystallization of the compatible PTHF-*b*-PMMA/PTHF blends were recently studied by using a synchrotron SAXS technique.[11] The crystallization of the crystallizable AB/A blends studied by the MacKnight and Nojima groups[8,9] was under the influence of "soft" amorphous microphases, meaning that the glass transition temperature (T_g) of the amorphous component was lower than the melting point (T_m) of the crystallizable component. The crystallization of our PTHF-*b*-PMMA/PTHF blends was under the influence of "hard" amorphous PMMA microphases, meaning that the T_g was higher than the T_m. These studies show that the "hard" amorphous microphases in our blends have a more significant effect on the crystallization behavior and crystalline morphologies than the "soft" rubbery microphases studied by other groups.

Our earlier study[10] shows that the crystallization behavior and morphology of the compatible and incompatible PTHF-*b*-PMMA/PTHF blends are very different. The compatible blends just have one melting peak, while the incompatible blends have two distinct melting peaks. The crystalline morphology of the compatible and incompatible PTHF-*b*-PMMA/PTHF blends are also very different. It changes very little with changes in blend composition for the incompatible blends but is very sensitive to blend composition for the compatible blends. And a few unusual crystalline morphologies were observed for the compatible blends, presumably due to the effect of dispersed "hard" PMMA amorphous microphases in the blends. The synchrotron SAXS study[11] on the microphase separation and crystallization of a series of compatible PTHF-*b*-PMMA/PTHF blends shows that the crystallization of the PTHF microphase has almost no effect on the original-phase separated structures in the amorphous state of the blend before

* Author to whom correspondence should be addressed at the present address: Department of Chemistry, State University of New York at Stony Brook, Stony Brook, New York 11794-3400.

[⊗] Abstract published in *Advance ACS Abstracts,* February 15, 1997.

S0024-9297(96)00684-5 CCC: $14.00

Table 1. Characteristics of PTHF-*b*-PMMA Diblock Copolymers and PTHF Homopolymer

designation[a]	M_n[b]	W[c](PTHF)	M_n(PTHF block)	M_n(PMMA block)
TM-A	17000	0.30	5100	11900
TM-B	8400	0.61	5100	3300
TM-C	23300	0.30	7000	16300
H-PTHF	2000	1.00		

[a] T and M denote abbreviations of PTHF and PMMA, respectively; H-PTHF = PTHF homopolymer. [b] M_n = number-average molecular weight. [c] W = weight fraction.

crystallization, including, for example, the PMMA interdomain distance. The unusual crystalline morphologies[10] of compatible PTHF-*b*-PMMA/PTHF blends were supposed to be resulting from the unchangeable microphase-separated structures during the crystallization process. In the present work, we concentrate our study on the crystallization kinetics and crystalline morphology of the compatible PTHF-*b*-PMMA/PTHF blends as a function of copolymer composition, the PTHF block length, blend composition, and crystalline conditions. The nonisothermal crystallization study shows that the crystallization temperature (T_c) on cooling, the melting point (T_m), and crystallinity (X_c) on subsequent heating changed appreciably with copolymer composition as well as blend composition. In particular, the crystalline morphologies of the blends changed remarkably with copolymer composition, blend composition, and crystallizable block length, although no dependence of T_c, T_m, and X_c on the crystallizable block length was observed within the molecular weight range we studied (from M_n = 5100−7000). The melt and solution crystalline morphologies of some of the blends are very different. Many very unusual crystallized morphologies were observed due to the effect of PMMA microdomains in the blends.

Experimental Section

Characterization of Polymers. The synthesis, purification, and characterization of tetrahydrofuran−methyl methacrylate diblock copolymer (PTHF-*b*-PMMA) were reported in previous papers.[10,12] A summary of the characteristics of the PTHF homopolymer and copolymers used in the present work is given in Table 1.

Preparation of Blends. The low molecular weight PTHF homopolymer listed in Table 1 was blended with the three PTHF-*b*-PMMA copolymers with different compositions and molecular weights in chloroform, a nonpreferential solvent for both blocks of the copolymer. The sample films of these blends and the pure copolymers were obtained by casting from the solution. They were then placed in a vacuum oven for one week at room temperature in order to remove residual solvent.

Differential Scanning Calorimetry (DSC). A Perkin-Elmer DSC-2c differential scanning calorimeter was used to study the crystallization of PTHF-*b*-PMMA diblock copolymers and PTHF-*b*-PMMA/PTHF blends. The DSC cooling thermograms of the samples were obtained at a rate of −10 K/min from 383 to 213 K, after the samples were annealed for 10 min at 383 K. The melting thermograms were obtained on a subsequent heating process at a rate of 10 K/min.

Polarized Optical Microscopy. A polarized optical microscope was used to study the crystalline morphology of the blends. The samples were cast from chloroform and then isothermally crystallized at 288 and 290 K, respectively. The melt-crystallized morphology was studied by quenching the sample films from melt (353 K) to 288 K after the films were dried in a vacuum oven for one week at room temperature. Since the crystallizability of the blends, whose major component is the copolymer, is much weaker than that of PTHF homopolymer, the crystalline time was set to 10 h to ensure that all the blends complete their crystallization. The micrographs of spherulite of the blends were taken with a 35-mm camera.

Table 2. DSC Results of PTHF-*b*-PMMA Diblock Copolymers and PTHF Homopolymer

designation	W(PTHF)	M_n(PTHF block)	T_c (K)	T_m (K)	X_c[a] (%)
TM-A	0.30	5100		287	16
TM-B	0.61	5100	263	297	33
TM-C	0.30	7000		289	18
H-PTHF	1.00	2000	277	296	55

[a] Crystallinity of PTHF block. $X_c = \Delta H/[W(\text{PTHF})\Delta H_m°]$.

Results and Discussion

1. Compatibility and Phase Behavior of the PTHF-*b*-PMMA/PTHF Blends. 1.1. Crystallization and Phase Behavior of the Neat PTHF-*b*-PMMA Diblock Copolymers. The SAXS studies[11,13] have shown that the copolymers used in the present work were microphase separated above the melting point of the PTHF block. The phase-separated structure of the TM-B copolymer[13] (Table 1) with a very low molecular weight (M_n = 8400) suggested the high incompatibility between PTHF and PMMA. The SAXS static[12] and dynamic[13] studies have also shown that regardless of whether the PTHF-*b*-PMMA block copolymer was cast from a solvent at room temperature or quenched from a disordered phase at high temperature to room temperature, the microphase separation between PTHF and PMMA always took place in advance of the PTHF crystallization. Therefore, it could be expected that the nucleation and the crystallization of the PTHF block of the copolymer could be retarded due to the restricted PTHF microphase dimensions. The DSC results of the copolymers TM-A, TM-B, and TM-C, as well as the PTHF homopolymer, are listed in Table 2. The crystallization temperature (T_c) listed in Table 2 was the temperature at the peak maximum of the crystallization peak of the sample upon cooling from 383 K to 213 K at a cooling rate of 10 K/min. The melting point (T_m) and the crystallinity (X_c) of the PTHF homopolymer and the PTHF block of the copolymer, were obtained on subsequent heating at a rate of 10 K/min. The enthalpy of fusion of PTHF with X_c = 1, $\Delta H_m°$ = 172.2 J/g,[14] was used to calculate the X_c of the PTHF block. As shown in Table 2, the T_c is 277 K for the neat PTHF homopolymer, while it is 263 K for the copolymer TM-B with 60 wt % of PTHF. The 14 K lower T_c of the copolymer than that of the homopolymer indicates that the nucleation and hence crystallization rate of PTHF in the PTHF microphase of the copolymer is much slower than those of the neat PTHF homopolymer. The X_c of the PTHF block in the TM-B copolymer was also much lower than that of the neat PTHF homopolymer (Table 2). The microphase separation between the PTHF and the PMMA blocks showed more appreciable effects on the crystallization of the PTHF block in the copolymers TM-A and TM-C with 30 wt % of PTHF than in the TM-B copolymer with 61 wt % of PTHF. No crystallization peak was observed during the same cooling process for the copolymers TM-A and TM-C, and only a small melting peak was observed during the subsequent heating. The T_m and X_c of the PTHF microphase in the copolymers TM-A and TM-C were also much lower than those in the TM-B copolymer, as listed in Table 2. The above DSC results about the three neat copolymers indicate that the crystallizability of the PTHF microphase decreases with decreasing of the PTHF content of the copolymer. The higher T_m and X_c of the TM-C

Table 3. Compositions of PTHF-*b*-PMMA/PTHF Blends

designation[a]	*W*(H-PTHF)	M_n(H-PTHF)	*W*(THF in blend)	*W*(H-PTHF in THF phase)
AT1 (CT1)	0.1	2000	0.37	0.27
AT2 (CT2)	0.2	2000	0.44	0.45
AT3 (CT3)	0.3	2000	0.51	0.59
AT4 (CT4)	0.4	2000	0.58	0.69
AT5 (CT5)	0.5	2000	0.65	0.77
AT6 (CT6)	0.6	2000	0.72	0.83
AT7 (CT7)	0.7	2000	0.79	0.89
AT8 (CT8)	0.8	2000	0.86	0.93
AT9 (CT9)	0.9	2000	0.93	0.97
BT1	0.1	2000	0.65	0.15
BT2	0.2	2000	0.69	0.29
BT3	0.3	2000	0.73	0.41
BT4	0.4	2000	0.77	0.52
BT5	0.5	2000	0.81	0.62
BT6	0.6	2000	0.84	0.71
BT7	0.7	2000	0.88	0.80
BT8	0.8	2000	0.92	0.87
BT9	0.9	2000	0.96	0.94
H-PTHF	1.0	2000	1.00	1.00

[a] The PTHF-*b*-PMMA copolymers in the AT, BT, and CT series of blends are TM-A, TM-B, and TM-C, respectively.

copolymer than those of the TM-A copolymer (Table 2) suggest that at a given copolymer composition the crystallizability of the PTHF microphase increases with increasing of the molecular weight of the PTHF block.

1.2. Compatibility and Phase Behavior of the PTHF-*b*-PMMA/PTHF Blends. Our previous study[10] on PTHF-*b*-PMMA/PTHF blends showed that the compatibility of the blend could easily be determined from its melting behavior. Just one PTHF melting peak was observed for the compatible blends. However, two distinct PTHF melting peaks were observed for the incompatible blends of the same polymer composition but with a higher homopolymer molecular weight, which rendered the blends incompatible. The higher melting peak of the incompatible blend could be attributed to the melting of PTHF in the homopolymer-rich macrophase, while the lower melting peak could be attributed to the melting of PTHF in the copolymer-rich macrophase. All three series of blends (Table 3) of a low molecular weight PTHF homopolymer ($M_n = 2000$) with the TM-A, TM-B, and TM-C copolymer, respectively, were compatible. The cast films in the melt states were transparent and showed one macroscopic phase under direct observation by optical microscope, in agreement with the DSC result showing only one melting peak.

The previous synchrotron SAXS study[11] of the CT series of compatible PTHF-*b*-PMMA/PTHF blends (Table 3) showed that all the blends containing 10%−90% PTHF homopolymer were microphase separated. The interdomain distance of the blend increased appreciably with increasing PTHF homopolymer weight fraction. The microphase morphologies of the CT series of blends in the melt state were determined on the basis of the multiple-order scattering peak positions from SAXS. The blends CT1 to CT3 with 10% to 30% PTHF homopolymer were confirmed to have an alternating PTHF and PMMA lamellar structure. The blends CT4 and CT5 with 40% and 50% PTHF homopolymer were confirmed to consist of a PTHF matrix with dispersed hexagonally packed PMMA cylinders. The SAXS profiles of the blends CT6 to CT9 with 60%−90% homopolymer did not exhibit enough higher-order scattering peaks to determine the PMMA microphase morphology of the blends. However, by considering the THF weight fraction of these blends, ranging from 0.72 to 0.93 (Table 3), the dispersed microdomains were likely to be made up of PMMA spheres. As listed in Table 3, the AT*i* ($i = 1, 9$) blend had the same polymer composition as that of the CT*i* ($i = 1, 9$) blend because the copolymers TM-A and TM-C had the same copolymer composition. Therefore, the AT*i* ($i = 1,9$) blend was likely to have the same microphase morphology as the CT*i* ($i = 1,9$) blend. Although the molecular weight of the neat TM-B copolymer contained in BT series of blends was relatively low ($M_n = 8400$), the copolymer was also confirmed by SAXS to be microphase separated both in the melt state and in the crystallized state[13] due to the high degree of incompatibility between PMMA and PTHF. Therefore, the microphase separation between PTHF and PMMA could be expected in the BT series of blends of the TM-B copolymer and the PTHF homopolymer. A SAXS investigation on a few selected homopolymer-rich blends from the BT series of samples confirmed that the blends were microphase-separated.

2. Nonisothermal Crystallization of the Compatible PTHF-*b*-PMMA/PTHF Blends. The SAXS study[11] of the CT series of blends also showed that PMMA microdomains (whether lamellar, cylindrical or spherical microdomains) remained essentially unchanged when the blend was crystallized from the melt. Moreover, the crystallization of the PTHF microphase did not show an obvious effect on the interdomain distance of the blend. Therefore, it could be expected that the presence of PMMA microdomains could have a great effect on the crystallization kinetics and the formation of the crystalline morphology of the blend. In the present work, the AT, BT, and CT series of PTHF-*b*-PMMA/PTHF blends (Table 3) were used to study the effects of the polymer composition of the blend and the PTHF block length of the copolymer on the crystallization behavior and the formation of the crystalline morphology of the blend. The THF weight fraction of the blend, which is the total weight fraction of the PTHF homopolymer and the PTHF block of the copolymer in a blend, is directly related to the microphase morphology of the blend, instead of the blend composition. The THF weight fraction, *W*(THF in blend); the PTHF homopolymer weight fraction, *W*(H-PTHF); and the PTHF homopolymer weight fraction in PTHF microphase, *W*(H-PTHF in THF phase) as well as the designation for each blend are listed in Table 3. *W*(H-PTHF in THF phase) was calculated on the basis of the strong segregation limit, where the PTHF homopolymer is assumed to be completely solubilized into the PTHF microdomains and

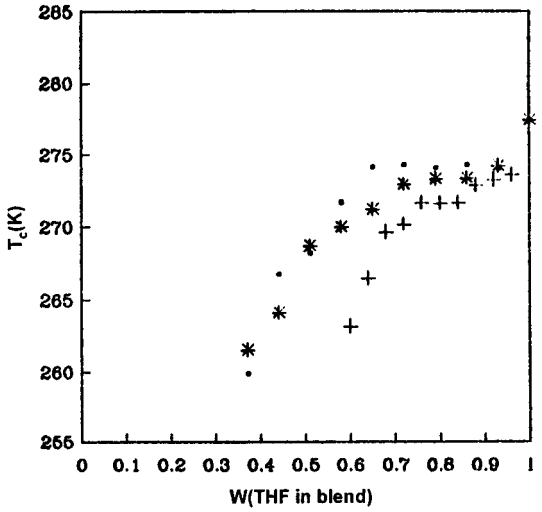

Figure 1. Nonisothermal crystallization temperature of the AT (●), BT (+), and CT (*) series of blends versus the THF weight fraction.

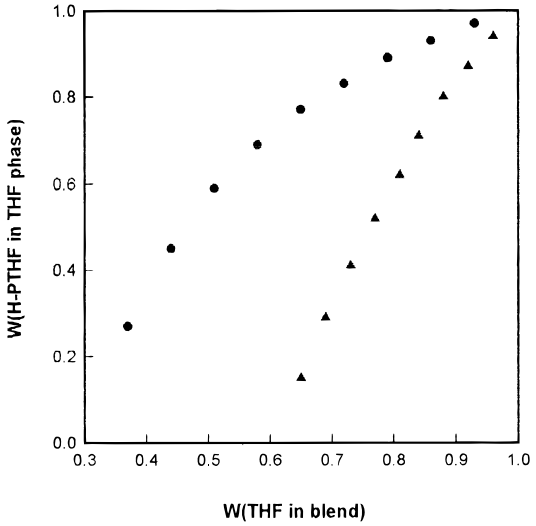

Figure 2. PTHF homopolymer weight fraction in the PTHF microphase versus the THF weight fraction of the AT (●), BT (▲) and CT (●) series of blends.

the PTHF block of the copolymer and the homopolymer are completely segregated from PMMA. Since the neat copolymer TM-B with 61% PTHF formed a PTHF matrix microphase, all of its blends with the PTHF homopolymer should have a PTHF matrix microphase. The CT series of blends with *W*(THF in blend) ≥ 0.58 were found to have a PTHF matrix microphase. Therefore, when the crystallization behavior and crystalline morphology are compared between BT series of blends and part of the CT series of blends, the comparison is based on that they all have a PTHF matrix microphase.

2.1. The Nonisothermal Crystallization Kinetics. Differential scanning calorimetry was used to study the nonisothermal crystallization kinetics of the three series of compatible PTHF-*b*-PMMA/PTHF blends. Upon cooling from 383 to 213 K at a cooling rate of 10 K/min, each blend showed a crystallization peak with a maximum position at T_c shown in Figure 1 as a function of the THF weight fraction. The T_c increased remarkably with increasing THF weight fraction up to *W*(THF in blend) = 0.75 for all the three series of blends. The SAXS study[11] of the CT series of blends showed that the interdomain distance of the blend increased from 29 to 79 nm with increasing THF weight fraction from 0.37 to 0.79, due to the solubilization of PTHF homopolymer into the PTHF microphase. The remarkable increase in T_c with increasing THF weight fraction of the blend, as shown in Figure 1, implies that the nucleation and hence the crystallization ability of the blend increase with increasing PTHF microphase size. Figure 1 also shows that, at a given THF weight fraction, the AT*i* (*i* = 1,9) and CT*i* (*i* = 1,9) blends have nearly the same T_c, indicating that the T_c of the blend is independent of PTHF block length, at least within our molecular weight range. However, at a given THF weight fraction, blend containing the most TM-A or the TM-C copolymer showed an appreciably higher T_c than the blend containing the TM-B copolymer, suggesting a T_c dependence of the blend on the copolymer composition. In fact, at a given THF weight fraction, the blend containing a copolymer with a higher PTHF content has less PTHF homopolymer in the PTHF microphase. Figure 2 shows the PTHF homopolymer weight fraction in the PTHF microphase [*W*(H-PTHF in THF phase)] versus the THF weight fraction [*W*(THF in blend)] for the three series of blends. The calculation of the *W*(H-PTHF in THF phase) was based on a strong segregation limit, i.e. all the homopolymer was solubilized in the PTHF microdomains. It is seen from Figure 2 that the *W*(H-PTHF in PTHF phase) increases sharply with increasing of the *W*(THF in blend) and that the blend containing the TM-B copolymer has much less PTHF homopolymer in the PTHF microphase than the blend containing the TM-A or TM-C copolymer at a given THF weight fraction. Therefore, the above T_c dependence of the blend on the copolymer composition implies that the more PTHF homopolymer the PTHF microphase contained, the greater the crystallizability. That is, the crystallizability of the PTHF block in the compatible PTHF-*b*-PMMA/PTHF blend was appreciably weaker than that of the PTHF homopolymer in the blend. Figure 1 also showed that all the blends with *W*(THF in blend) ≥ 0.85 had approximately the same crystallization temperature (T_c). However, the T_c of these blends was appreciably lower than that of the neat PTHF homopolymer. For example, the BT1 blend containing only 3.9% PMMA had an about 3.5 K lower T_c than the neat PTHF homopolymer. This finding indicated that a very small amount of the PMMA microdomains could appreciably retard the nucleation and hence the crystallization of the PTHF homopolymer in the compatible PTHF-*b*-PMMA/PTHF blend.

2.2. Melting Behavior. The melting data point in Table 2 and Figure 3 was obtained during a heating process (10 K/min), subsequent to the crystallization process described in the above section. Because of a higher molecular weight of the PTHF prepolymer (M_n = 5100) of the copolymers TM-A and TM-B than the H-PTHF homopolymer (M_n = 2000) used in the blends, the PTHF prepolymer has a higher T_m than the H-PTHF homopolymer. As seen in Table 2, the T_m of the copolymers having the PTHF prepolymer as one of the blocks could be still higher than that of the H-PTHF homopolymer, but could also be lower than that of the homopolymer, depending on the copolymer composition. The TB-A copolymer with 30 wt % of PTHF had a 9 K lower T_m than the homopolymer H-PTHF, while the TM-B copolymer with 60 wt % of PTHF had a higher T_m than the homopolymer. The remained high T_m of the TM-B copolymer is attributed to the formation of a PTHF-matrix, and the low T_m of the TM-A copolymer is attributed to the formation of PTHF dispersed microphase. Similarly, all the blends containing the TM-B

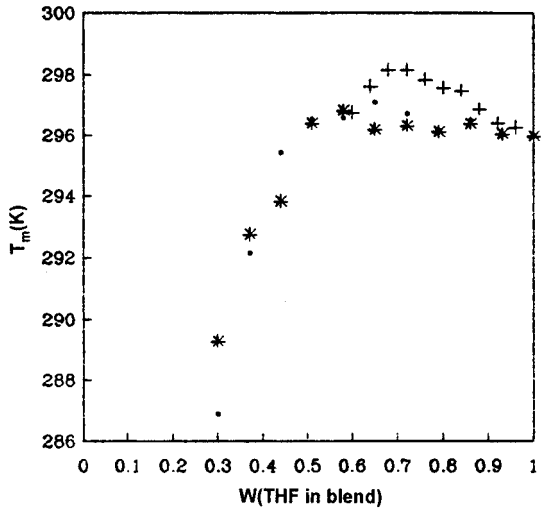

Figure 3. The melting temperature of the AT (•), BT (+), and CT (*) series of blends versus the THF weight fraction.

copolymer had a PTHF matrix, and thus they all showed a higher T_m than the H-PTHF homopolymer, as shown in Figure 3. Moreover, the blends BT1 and BT2 with 10% and 20% PTHF homopolymer showed an even higher T_m than the neat TM-B copolymer (Figure 3), presumably due to the increase of the crystallizability of the PTHF block after the PTHF microphase was solubilized by a small amount of low molecular weight PTHF homopolymer. The previous SAXS study[11] showed that the blends CT1 to CT3 with the THF weight fraction from 0.37 to 0.51 had an alternating PTHF and PMMA lamellar structure. The average thickness of the PTHF lamellae of the blends CT1, CT2, and CT3 were 12.2, 15.1, and 19.5 nm, respectively, which were comparable to the magnitude (17 nm) of the long period of the neat PTHF homopolymer under the same crystallization condition. The melting point (T_m) of the PTHF lamellar microphase increased sharply with increasing THF weight fraction for the three blends, as shown in Figure 3, suggesting that the crystallization behavior of this confined PTHF microphase was very sensitive to the PTHF lamellar thickness. The CT3 blend, with the thickness (19.5 nm) of the PTHF lamellar microphase being larger than the magnitude (17 nm) of the long period of the neat PTHF homopolymer under the same crystallization condition, showed the same melting point as the neat PTHF homopolymer. The AT*i* (i = 1,9) blend had the same polymer composition as the CT*i* (i = 1,9) blend (see Table 3); therefore, the blends AT1 to AT3 likely had an alternating PTHF and PMMA lamellar structure in the amorphous state, but presumably with a thinner average PTHF lamella than that of the CT*i* blend due to the lower molecular weight of the TM-A copolymer than that of the TM-C copolymer. The blends AT1 to AT3 also exhibited a sharp increase in T_m with increasing of the THF weight fraction, and the AT3 blend reached the same T_m as the neat PTHF homopolymer, as shown in Figure 3. The CT*i* (i = 4, 9) blends with 40 wt % or more of PTHF homopolymer were confirmed[11] to have a PTHF matrix microphase, and these blends as well as AT*i* (i = 4,9) blends had nearly the same melting point as the H-PTHF homopolymer, as also shown in Figure 3.

The size increase of the PTHF microphase could be partly responsible for the T_m increase of the blends AT*i* (i = 1, 3) and CT*i* (i = 1, 3). The rapid increase in T_m of these blends with increasing THF weight fraction could also be partly due to the increase of the PTHF homopolymer weight fraction in the PTHF microphase, because the PTHF homopolymer would have less conformational constraint than the PTHF block of the copolymer and thus have a stronger crystallizability than the PTHF block. A recent small angle neutron scattering (SANS) study[15] confirmed that a homopolymer in lamellar microdomains of a blend with a block copolymer have an undisturbed conformation, at least in the direction parallel to the lamellae. The much higher T_m of the CT1 and AT1 blends with only 10 wt % of the PTHF homopolymer than that of their corresponding neat copolymers (Figure 3) indicates that the solubilization of the PTHF homopolymer into the PTHF microphase can greatly improve the crystallizabilty of the microphase.

2.3. Crystallinity of the PTHF Microphase. The degree of crystallinity of the PTHF microphase of the neat copolymers TM-A, TM-B, and TM-C was much lower than that of the neat PTHF homopolymer due to the microphase separation of the copolymers, as listed in Table 2. In the blend of the copolymer with the low-molecular weight PTHF homopolymer, the crystallizability of the PTHF microphase increased with increasing homopolymer weight fraction, resulting in the increase in the T_c and the T_m of the PTHF microphase with addition of the PTHF homopolymer (Figures 1 and 3). The improved crystallizability of the PTHF microphase of the blend also had an appreciable effect on the crystallinity of this phase, as shown in Figure 4. The crystallinity X_c of PTHF micophase of the blend was calculated from the following equation:

$$X_c = \Delta H/[(W(\text{THF in blend}) \times \Delta H_m^\circ)] \qquad (1)$$

where ΔH is the enthalpy of fusion of the blend on the subsequent heating process and ΔH_m° is the enthalpy of fusion of PTHF with $X_c = 1$. The three series of blends exhibited a constant increase in X_c with increasing of the THF weight fraction, unlike the melting behavior of AT and CT series of blends showing a sharp increase in T_m as the THF weight fraction increased from 0.37 to 0.51 but showing no more change in T_m with further increasing of the THF weight fraction. Moreover, regardless of the percentage of the homopolymer in the PTHF microphase, the X_c of the microphase was always lower than that of the neat PTHF homopolymer, presumably resulting from the lower crystallinity of the PTHF block of the copolymer than that of the PTHF homopolymer solubilized into the PTHF microphase. This supposition on lower crystallinity of the PTHF block than the PTHF homopolymer in the PTHF microphase was confirmed by the fact that at a given THF weight fraction the X_c of the blend containing copolymer TM-B with high PTHF content (61%) was appreciably lower than that of the blend containing the TM-A or TM-C copolymer with low PTHF content (30%), as shown in Figure 4. Since the TM-A and TM-C copolymers had a same copolymer composition but different PTHF block length, the nearly same crystallinity dependence on the THF weight fraction for the AT and the CT series of blends suggested that the molecular weight of the PTHF block did not have an appreciable effect on the crystallinity of the PTHF microphase of the blend, at least within our molecular weight range.

2.4. Cocrystallization of the PTHF Homopolymer and the PTHF Block in the THF Microphase. Upon cooling from the melt, the neat PTHF-*b*-PMMA copolymer and the PTHF homopolymer crystallized at

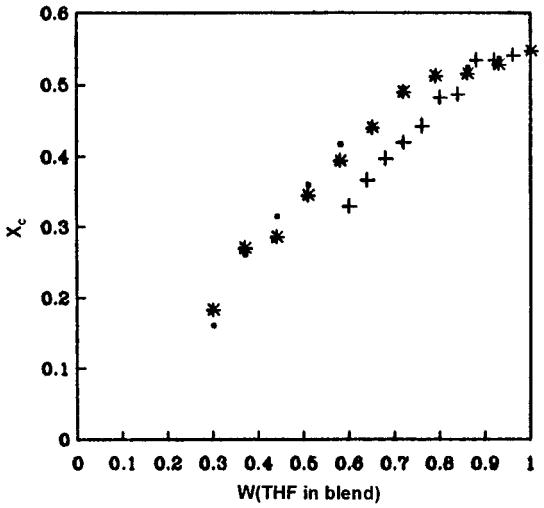

Figure 4. Crystallinity degree of the AT (●), BT (+), and CT (*) series of blends versus the THF weight fraction.

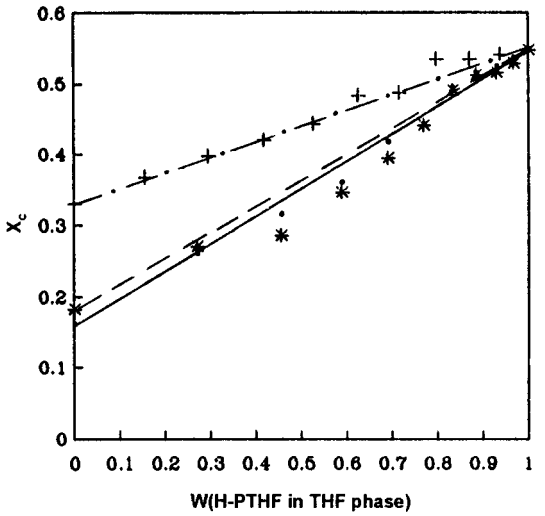

Figure 5. The crystallinity degree of the AT (●), BT (+) and CT (*) series of blends versus the PTHF homopolymer weight fraction in the PTHF phase and calculated crystallinity degrees of the AT (—), BT (-●-) and CT (- - -) series of blends under the assumption that the PTHF homopolymer and the PTHF block had the same crystallinity degrees as the pure homopolymer and the neat copolymer, respectively.

very different temperatures, such as the copolymer TM-B and the homopolymer showing the T_c at 263 and 277 K, respectively. The melting points of the copolymer and homopolymer on the subsequent heating process also could be very different, such as the copolymer TM-A and the homopolymer showing T_m at 287 and 296K (Table 2), respectively. In a previous DSC study,[10] it was found that an incompatible PTHF-*b*-PMMA/PTHF blend showed one or two crystalline peaks on cooling and two distinct melting peaks on subsequent heating. The higher T_c and T_m of the incompatible blend were attributed to the macrophase of PTHF homopolymer in the blend, while the lower T_c and T_m were attributed to the copolymer-rich macrophase. However, for the compatible PTHF-*b*-PMMA/PTHF blends, only one T_c and one T_m were exhibited on the same cooling and heating processes. The three series of blends studied in this work were all compatible and exhibited only one T_m. This crystallization feature of the compatible PTHF-*b*-PMMA/PTHF blend implies that the PTHF block can crystallize together with the homo-PTHF in the PTHF microdomains. The T_c of the blend with the homopolymer as the major component could be 12 K higher than that of the neat copolymer, as shown in Figure 1, indicating that the PTHF block could cocrystallize with the PTHF homopolymer at a much higher temperature than the neat copolymer. The cocrystallization behavior could be confirmed by quantitatively analyzing the crystallinity of the PTHF microphase of the blend. The crystallinity of the blend is shown in Figure 5 as a function of homo-PTHF weight fraction in the PTHF microphase, together with the calculated X_c of the blend, based on the the assumption that the PTHF homopolymer and PTHF block retained the same crystallinity degrees as the neat homopolymer and the neat copolymer, respectively. It is seen that the calculated X_c fit the experimental data well, especially for BT series of blends. This means that if we assume the PTHF block did not cocrystallize with the homo-PTHF in the PTHF microphase, the crystallinity of the PTHF homopolymer could be much higher than that of the neat homo-PTHF, possibly even over 100%. Obviously, this is unreasonable, and it can be concluded that the enthalpy of fusion of the blend is attributed to the crystals consisting of both the PTHF homopolymer and the PTHF block in the PTHF microphase.

3. Intriguing Crystalline Morphologies. 3.1. Isothermal Crystalline Morphologies from the Melt. The SAXS study[11] of the CT series of blends demonstrates that the PMMA microdomains (whether lamellar, cylindrical, or spherical microdomains) remain essentially unchanged when the blend is crystallized from the melt. Moreover, the crystallization of the PTHF microphase did not show an obvious effect on the average interdomain distance of the blend. Therefore, it could be expected that the presence of PMMA microdomains could have an appreciable effect on the formation of the crystalline morphology of the blend. When the CT series of blends were isothermally crystallized at 288 K from the melt (353 K), the crystalline morphology changed dramatically with blend composition, as shown in Figure 6. The blends CT1, CT2, and CT3 were confirmed to have an alternating PTHF and PMMA lamellar structure with an average PTHF lamellar thickness of 12.2, 15.1, and 19.5 nm, respectively.[11] No macroscopic crystalline morphology was observed for blends CT1 and CT2, and only small macroscopic crystals were observed for the CT3 blend. This indicates that only when the PTHF lamellar thickness is large enough, say 20 nm, will the blend form the crystals that are observable with a polarized optical microscope. The blends CT4 and CT5 were confirmed to have the PTHF matrix microphase with hexagonally packed PMMA cylinders. The blends CT6 to CT9 were found to have a PTHF matrix but were likely dispersed with PMMA spheres. Unlike the CT3 blend, the CT4 blend exhibited the typical spherulite structure with a familiar maltese cross birefringent pattern. The spherulitic size of the CT4 blend was much larger than the crystal size of the CT3 blend. This infers that crystal growth in the PTHF matrix microphase is much easier than in the PTHF lamellar microphase. The blends CT5 and CT6 exhibited a similar crystalline morphology, as shown in Figure 6 for the CT6 blend, for example. The spherulitic morphology of the CT6 blend was different from that of the CT4 blend. The blends CT7 and CT8 formed very unusual crystalline morphologies. The CT9 blend with 10 wt % of the TM-C copolymer formed spherulites with regular extinction rings. The neat PTHF homopolymer formed small immature spherulites under the same crystallization condition. The above results indicate

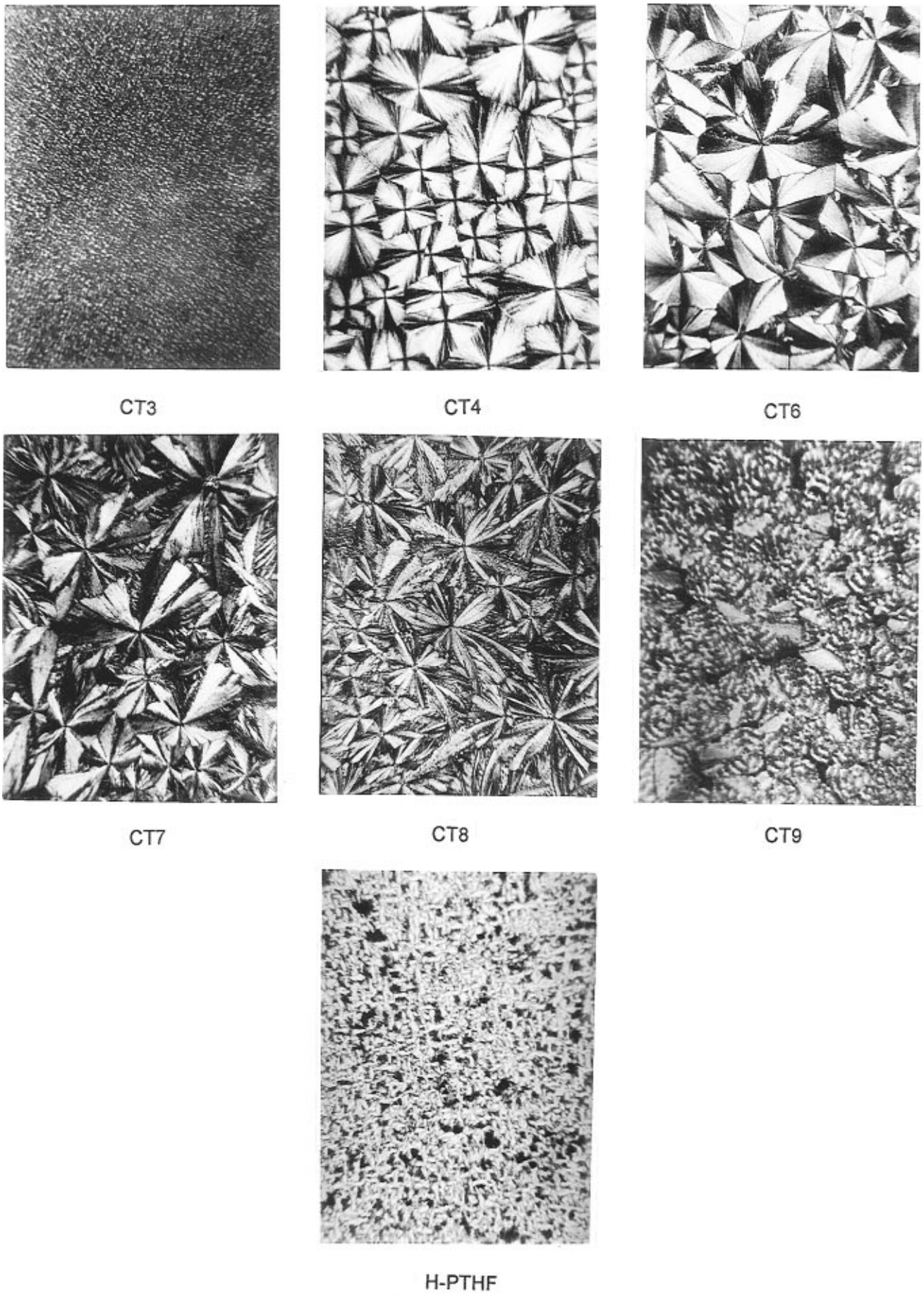

Figure 6. Crystalline morphologies of the CT series of blends crystallized at 288 K from the melt (magnification 375×).

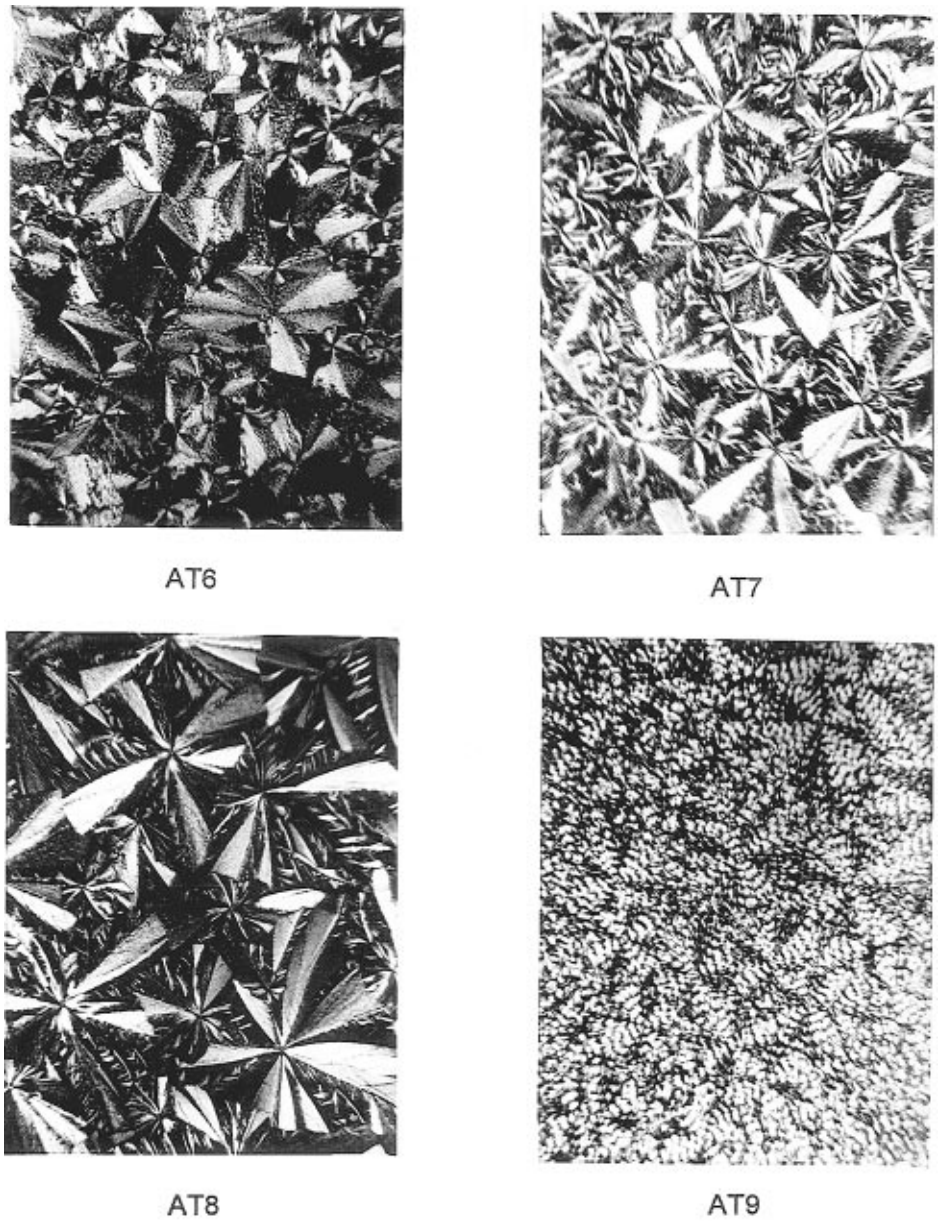

Figure 7. Crystalline morphologies of the blends AT6 to AT9 crystallized at 288 K from the melt (magnification 375×).

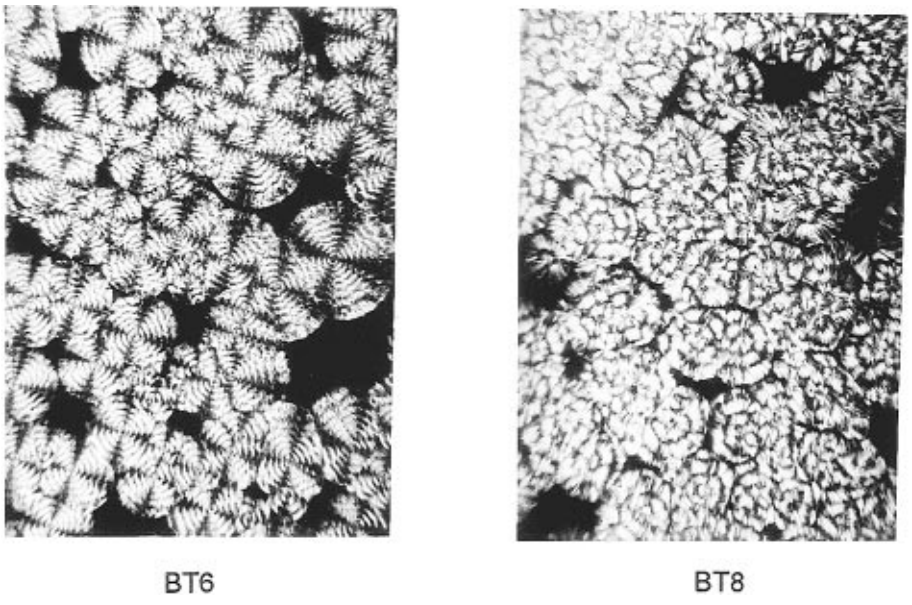

Figure 8. Crystalline morphologies of the BT6 and BT8 blends crystallized at 288 K from the melt (magnification 375×).

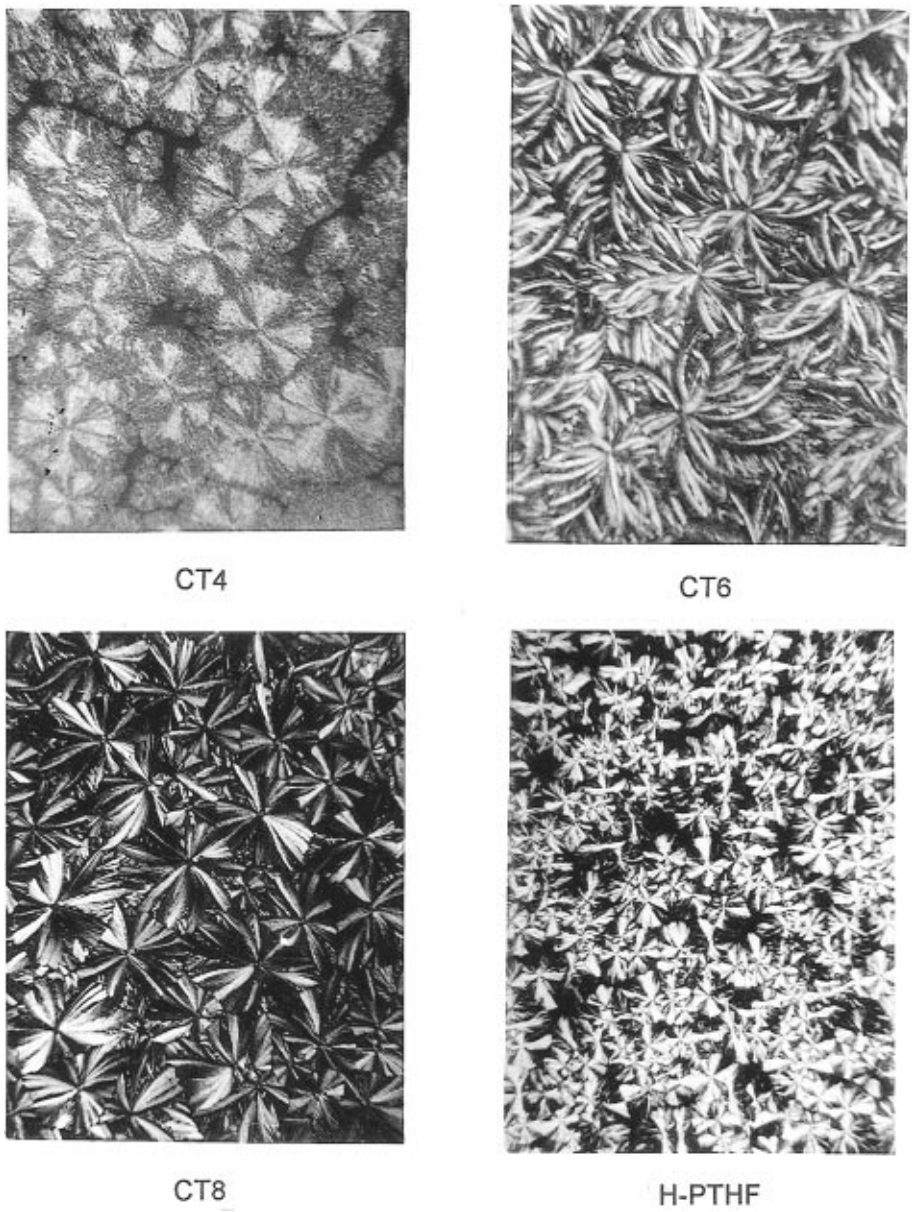

Figure 9. Crystalline morphologies of some of the CT series of blends cast from chloroform at 288 K (magnification 375×).

that when the PTHF matrix microphase was formed in the blend, the crystalline morphology changed dramatically with the copolymer weight fraction. It is believed that the copolymer weight fraction governs the PMMA microphase morphology (cylinder and sphere) and the interdomain distance. The SAXS study[11] shows that the PMMA cylinder radius and the interdomain distance in the CT4 blend were 14.7 and 46 nm, respectively, while the PMMA sphere radius and the interdomain distance in the CT7 blend (assuming it has body-centered cubic symmetry) were 25.5 and 79.4 nm, respectively. Therefore, it is clear that the dispersed PMMA microdomain morphology, the microdomain size, and the interdomain distance have a dramatic effect on the formation of the crystalline morphology of the compatible PTHF-*b*-PMMA/PTHF blends. The much bigger spherulites observed in the blends than in the pure PTHF homopolymer indicate an appreciable decrease in nucleation density due to the presence of the PMMA microdomains. However, the spherulites of the blends do not become progressively larger with increasing of the copolymer weight fraction.

The AT*i* ($i = 1, 9$) blend, having the same polymer composition as the CT*i* ($i = 1, 9$) blend, was expected to have the same microphase morphology as the CT*i* ($i = 1, 9$) blend. The DSC nonisothermal crystallization study showed that the AT and CT series of blends exhibited nearly the same crystallization behavior on cooling and subsequent heating, as shown in Figures 1, 3, and 4. Some of the AT series of blends had melt crystallized morphologies similar to those of the CT series of blends; for example, both the AT9 and CT9 blends formed the ringed spherulites with only a slight difference in band spacing of the banded structure, as shown in Figures 6 and 7. However, most of the AT series of blends formed very different melt crystalline morphologies than the CT series of blends, such as the blends AT*i* ($i = 6, 8$) and CT*i* ($i = 6, 8$) also shown in Figures 6 and 7. Since the TM-A copolymer contained in the AT series of blends had a shorter PMMA block than the TM-C copolymer contained in the CT series of blends, the PMMA microdomain size and interdomain distance of the AT*i* ($i = 1, 9$) blend were expected to be smaller than those of the CT*i* ($i = 1, 9$) blend. The large differences in crystalline morphology between some of the AT and CT series of blends presumably resulted from the differences in the PMMA microdomain size and the interdomain distance.

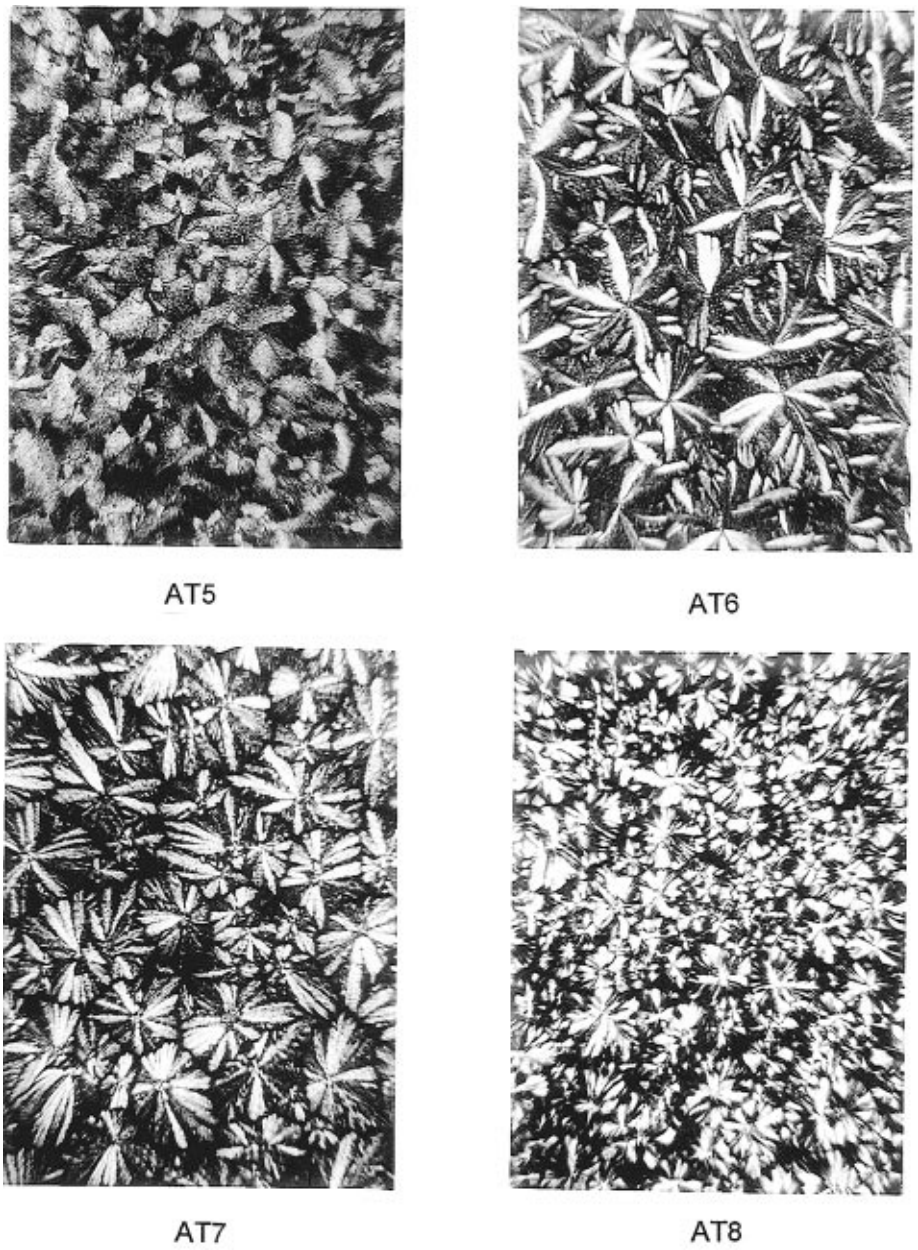

Figure 10. Crystalline morphologies of the blends AT5 to AT8 cast from chloroform at 288 K (magnification 375×).

The PTHF matrix microphase was formed in all the BT series of blends due to the high PTHF content of the TM-B copolymer. A ringed spherulite structure (or a banded structure) was observed for most of the BT series of blends (BT4 to BT8), as shown in Figure 8 for the BT6 and BT8 blends for example. Banded structures in polymeric spherulites are believed to arise from cooperative twisting of radiating lamellar crystals about their axis of fastest growth.[16] The twisting of the PTHF lamellae in the compatible PTHF-*b*-PMMA/PTHF blend is supposed to be attributed to the presence of the PMMA microdomains. The BT8 blend with W(THF in blend) = 0.92 as well as the blends AT9 and CT9 with W(THF in blend) = 0.93 formed ringed spherulites, while the BT9 blend with W(THF in blend) = 0.96 did not form this morphology. This indicates that only when the PMMA weight fraction of the blend is above a critical value, say 7%, will the ringed spherulite be formed. The morphology study about the BT series of blends also shows that the band spacing of the ringed spherulites becomes progressively larger with decreasing of the copolymer content (or the amorphous PMMA content), as seen in Figure 8 for the BT6 and BT8 blends with 40% and 20% copolymer, respectively. This dependence of the band spacing on the amorphous PMMA content is consistent to literature findings that the band spacing usually decreases upon addition of noncrystalling diluents (but increases with crystallization temperature).[16,17] Unlike other polymeric systems, the amorphous PMMA content in our block copolymer/homopolymer blends forms microdomains. The PMMA interdomain distance also decreases with decreasing of the copolymer weight fraction. The same dependence of the PMMA microdomain interdistance and the band spacing on the copolymer weight fraction suggests that the PMMA interdomain distance plays an important role in the formation of the banded structure. The smaller the PMMA interdomain distance, the more the PTHF lamellae twist and the smaller the band spacing of the ringed spherulites. At a similar W(THF in blend) fraction, the blend containg the TM-B copolymer could also be expected to form a different crystalline morphology than the blend containing the TM-A or the TM-C copolymers, due to the differences in the molecular

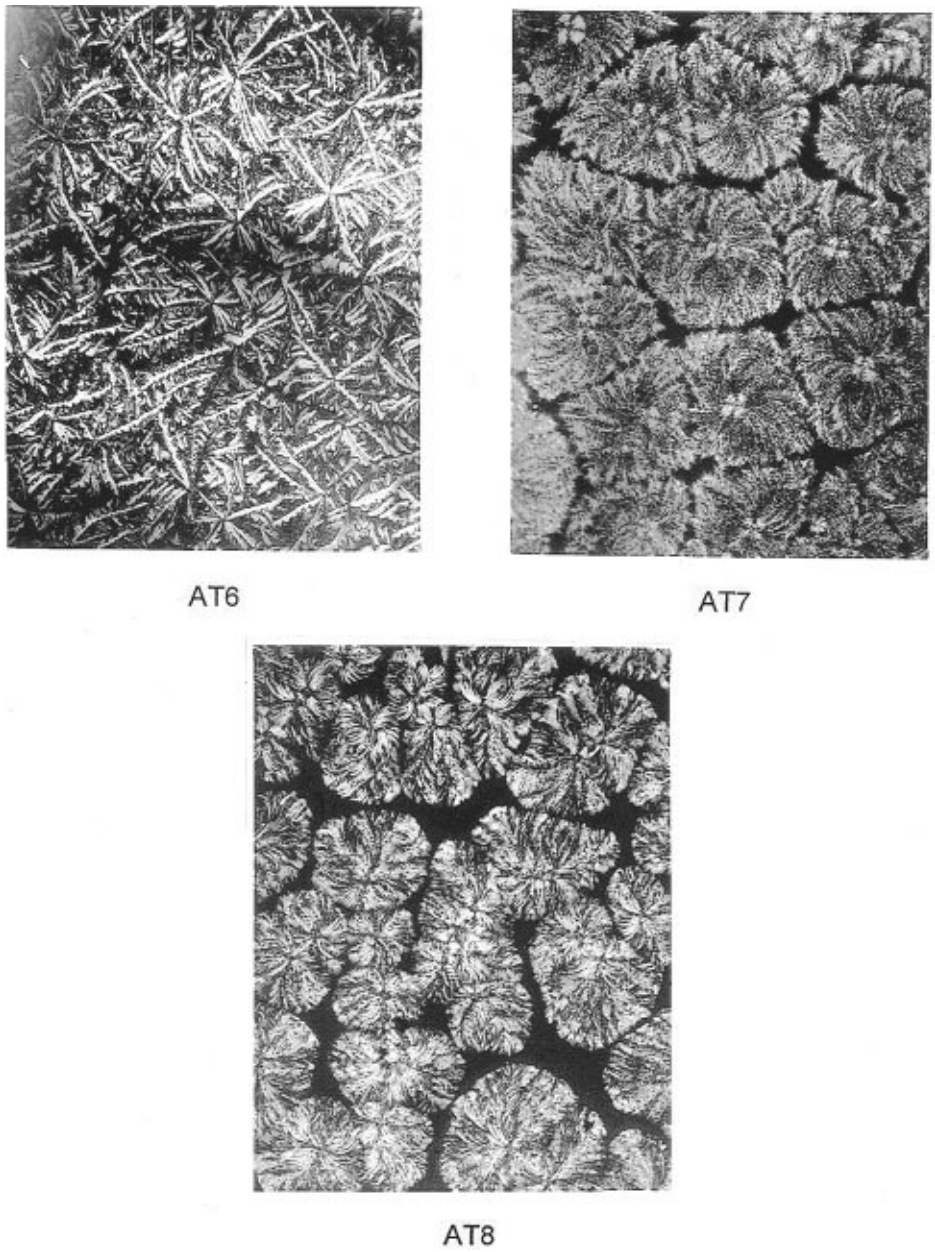

Figure 11. Crystalline morphologies of the blends AT6 to AT8 cast from chloroform at 290 K (magnification 375×).

weight and the copolymer composition of these copolymers. The blends BT4 to BT7 with *W*(THF in blend) values from 0.77 to 0.88 had the ringed spherulite, while the blends AT7, CT7, AT8, and CT8 with the similar *W*(THF in blend) values of 0.79 and 0.86 formed the very unusual crystalline morphologies shown in Figures 6 and 7, respectively. The molecular weight of the PMMA block of the TM-B copolymer is about 3 times smaller than that of the TM-A copolymer and 5 times smaller than that of the TM-C copolymer (Table 1). This difference in the PMMA block length of the copolymers can lead to a large difference in the PMMA domain size and the interdomain distance for the three series of blends. At a given *W*(THF in blend) fraction, both the PMMA domain size and the interdomain distance of the blend containing the TM-B copolymer are supposed to be smaller than that of the blend containing the TM-A or the TM-C copolymer. The very different crystalline morphology of the blend containing the TM-B copolymer compared to the blend containing the TM-A or the TM-C copolymer at a similar *W*(THF in blend) fraction presumably resulted from the difference in the PMMA microdomain size and the interdomain distance.

3.2. Isothermal Crystalline Morphologies from Solution and Their Temperature Dependence. The crystalline morphology of the blends was also studied by casting the solutions in a nonselective solvent, $CHCl_3$. The samples were cast and crystallized at 288 K. The only difference observed between the melt- and solution-crystallized morphologies of the pure PTHF homopolymer was the spherulitic size (see Figures 6 and 9). However, most of the blends exhibited a very different crystallized morphology from the melt-crystallized morphology, such as the CT4, CT6, and CT8 blends (see Figures 6 and 9) as well as the AT5 to AT8 blends (see Figures 7 and 10). The flowerlike solution-crystallized morphology of the CT6 blend with 60% PTHF homopolymer shown in Figure 9 was very different from its melt-crystallized morphology shown in Figure 6. The AT5 blend with 50% homopolymer formed a ringed spherulite structure from melt (not shown), but exhibited an intringuing crystalline morphology when crys-

tallized from solution (see Figure 10). The AT9 blend with 90% homopolymer also formed the ringed spherulite from melt (see Figure 7), but it did not form the same morphology when cast from solution. The crystalline morphologies of the AT6 and AT7 blends with 60% and 70% homopolymer were very unusual when the blends were crystallized from solution, as shown in Figure 10. The ringed spherulite structure observed for the BT4 to BT8 blends with 40% to 80% homopolymer, respectively, was only observed for the BT5 and BT6 blends when the blends were cast from solution.

The direct observation showed that, when cast from the solvent, the blend started crystallizing well after the bulk film was formed, implying that the microphase separation of the blend took place well in advance of the PTHF crystallization.[12] The SAXS study of the CT series of blends showed that the main difference between the scattering behavior of the cast blend film and the subsequent annealed film was the absence of the higher order scattering peaks for the cast film, suggesting that the microdomain packing in the cast sample was less regular than in the annealed sample. This difference in PMMA microdomain packing was not supposed to result in an appreciable difference between the solution and the melt crystallization behavior of the blend. However, a very small amount of residual solvent in the cast film could appreciably slow down the nucleation and hence the crystallization rate. Therefore, the very different solution- and melt-crystallized morphologies of the compatible PTHF-*b*-PMMA/PTHF blend could have been caused by the different crystallization rates. That is, under different crystallization rates, the PMMA microdomains could have different effects on the crystalline morphology formation. This supposition on the morphology dependence on crystallization rate was confirmed by the fact that very different crystalline morphologies of the blend were observed when cast and crystallized at different temperatures. As shown in Figures 10 and 11, the AT6 to AT8 blends formed very different crystalline morphologies when cast at 288 and 290 K, respectively.

Irrespective of whether the blends were crystallized from melt or solution, the PMMA microdomain played a role in restricting nucleation for PTHF crystallization, as manifested by the large increase in PTHF spherulitic size with addition of the copolymer (see Figures 6 and 9). This morphological feature is in agreement with the DSC results showing an appreciable decrease in the crystallization temperature (T_c) with addition of the copolymer shown in Figure 1.

Conclusions

(1) The DSC nonisothermal crystallization study shows that the crystallizability of the PTHF microphase in the blend increases with increasing of the PTHF microphase size and the PTHF homopolymer weight fraction in the PTHF microphase and that regardless of the percentage of the homopolymer in the PTHF microphase, the degree of crystallinity of the PTHF block is always lower than that of the PTHF homopolymer.

(2) A very small amount of PMMA microdomains can appreciably retard the nucleation and hence the crystallization of the PTHF homopolymer in the compatible PTHF-*b*-PMMA/PTHF blends, as evidenced by an appreciably lower T_c and much larger spherulites of the blends with 10 wt % of the copolymers (~3.9−7.0 wt % of PMMA) than those of the pure PTHF homopolymer.

(3) When the PTHF matrix microphase was formed in the blend, this phase had approximatly the same melting point as that of the neat PTHF homopolymer, while when the alternating PTHF and PMMA lamellar microphase were formed, the melting point of the PTHF lamellae decreased with decreasing of the THF weight fraction of the blend.

(4) When the alternating PTHF and PMMA lamellae were formed, the macroscopic crystalline morphology could be only observed when the thickness of PTHF lamellae was large enough (~20 nm). When the PMMA spherical or cylindrical microphase were formed, the crystalline morphology changed remarkably with changes in the interdomain distance and the domain size, and many unusual crystalline morphologies were observed.

(5) The crystalline morphology of the compatible PTHF-*b*-PMMA/PTHF blend also exhibited a strong dependence on isothermal solution crystallization temperatures, which govern the crystallization rate. This indicates that, under different crystallization rates, the PMMA microdomains have different effects on the formation of the solution-crystallized morphology of the blend.

Acknowledgment. L.L. gratefully acknowledges support of this work by Young Investigator Grant, Chinese Academy of Sciences and by National Basic Research Project−Macromolecular Condensed State.

References and Notes

(1) Tanaka, H.; Hasegawa, H.; Hashimoto, T. *Macromolecules* **1991**, *24*, 240.
(2) Winey, K. I.; Thomas, E. L.; Fetters, L. J. *Macromolecules* **1992**, *25*, 2645.
(3) Jeon, K.-J.; Roe, R.-J. *Macromolecules* **1994**, *27*, 2439.
(4) Zhao, J.; Majumdar, B.; Schulz, M. F.; Bates, F. S.; Almdal, K.; Mortensen, K.; Hajduk, D. A.; Gruner, S. M. *Macromolecules* **1996**, *29*, 1204.
(5) Matsen, M. W. *Macromolecules* **1995**, *28*, 5765
(6) Whitmore, M. D.; Noolandi, J. *Macromolecules* **1985**, *18*, 2486.
(7) Olvera de le Cruz, M.; Sanchez, I. *Macromolecules* **1987**, *20*, 440.
(8) Sakurai, K.; MacKnight, W. J.; Lohse, D. J.; Schulz, D. N.; Sissano, J. A. *Macromolecules* **1994**, *27*, 4941.
(9) Nojima, S.; Takahashi, Y.; Ashida, T. *Polymer*, **1994**, *35*, 2853.
(10) Liu, L.-Z.; Li, H.; Jiang, B.; Zhou E. *Polymer* **1994**, *35*, 5511.
(11) Liu, L.-Z.; Yeh, F.; Chu, B. *Macromolecules* **1996**, *29*, 5336.
(12) Liu, L.-Z.; Jiang, B.; Zhou, E. *Polymer* **1996**, *37*, 3937.
(13) Liu, L.-Z.; B. Chu, to be published.
(14) Dreyfuss, P. *Poly(tetrahydrofuran)*; Gordon and Breach: New York, 1982.
(15) Matsushita, Y.; Torikai, N.; Mogi, Y.; Noda, I.; Han, C. C. *Macromolecules* **1994**, *27*, 4566.
(16) Keith, H. D.; Padden, F. J., Jr.; Russell, T. P. *Macromolecules* **1989**, *22*, 666.
(17) Pizzoli, M.; Scandola, M.; Cerrorulli, G. *Macromolecules* **1994**, *27*, 4755.

MA960684O